

Chapter

3

Identification of (1→4)-linked α -glucooligomers in cell-wall α -glucan of fission yeast

Christian H. Grün¹, Frans Hochstenbach², Frans M. Klis³, Johannis P. Kamerling¹, and Johannes F.G. Vliegthart¹

¹Bijvoet Center, Department of Bio-Organic Chemistry, Section of Glycoscience and Biocatalysis, Utrecht University; ²Department of Biochemistry, Academic Medical Center, University of Amsterdam; ³Swammerdam Institute for Life Sciences, University of Amsterdam

Abstract

The cell wall of fission yeast mainly consists of two types of polysaccharides, namely β -glucan and α -glucan. Previously, we have described the structure of fission-yeast α -glucan and concluded that it consists of two building blocks, each composed of a (1 \rightarrow 3)- α -glucan segment of approximately 135 α -glucose residues linked to a short stretch containing (1 \rightarrow 4)-linked residues. However, it remained unclear whether this stretch is a homooligosaccharide of (1 \rightarrow 4)-linked α -glucose or whether it is composed of alternating (1 \rightarrow 3)-linked and (1 \rightarrow 4)-linked glucose residues. Here, we describe the chemical structure of the stretch containing (1 \rightarrow 4)-linked glucose residues by digesting α -glucan with a (1 \rightarrow 3)- α -glucanase preparation and the elucidation of the reaction products by nano-electrospray mass spectrometry. We identified two classes of oligosaccharides, namely one class comprising heterooligosaccharides consisting of a number of consecutive (1 \rightarrow 4)-linked α -glucose residues linked to a number of (1 \rightarrow 3)-linked α -glucose residues, and a second class consisting of consecutive (1 \rightarrow 4)-linked α -glucose, only. We propose that the first class originates from the center part of the α -glucan, whereas the second class forms the reducing end. These data demonstrate that each (1 \rightarrow 3)- α -glucan segment is covalently linked to a homooligomer of (1 \rightarrow 4)-linked α -glucose residues.

Introduction

The cell wall of many fungi is composed of three types of polysaccharides, namely chitin, β -glucan and α -glucan. Although the first two types have been studied thoroughly, little is known about the chemical structure and biosynthesis of α -glucan. In fission yeast, *Schizosaccharomyces pombe*, α -glucan was identified by Bacon and co-workers (1968) and its chemical composition was determined by Bush and co-workers (1974), who concluded that it consisted mainly of (1 \rightarrow 3)-linked α -glucose residues with some (1 \rightarrow 4)-linked residues. Recently, we determined that these (1 \rightarrow 4)-linked residues are an integral part of cell-wall α -glucan. We showed that α -glucan is a linear polysaccharide composed of two covalently coupled building blocks, each comprising a linear (1 \rightarrow 3)- α -glucan segment of approximately 135 residues linked to a stretch containing a number of (1 \rightarrow 4)-linked glucose residues. Importantly, α -glucan from a mutant that is defective in α -glucan synthesis consisted of a single building block, only (Chapter 2). We proposed a model for the biosynthesis of α -glucan in which we postulated that the (1 \rightarrow 4)-linked glucose residues might form a primer molecule, necessary for the initiation of α -glucan synthesis.

The use of an oligosaccharide primer for polysaccharide biosynthesis is not unusual. For example, for the synthesis of (1 \rightarrow 3)- α -glucan produced by *Streptococcus mutans*, a primer composed of (1 \rightarrow 6)-linked α -glucose residues is required (Germaine *et al.*, 1974) and cellulose biosynthesis is initiated by a (1 \rightarrow 4)- β -glucooligosaccharide (Peng *et al.*, 2002), whereas the synthesis of glycogen and starch requires a (1 \rightarrow 4)- α -glucooligomer as a primer (Alonso *et al.*,

1995; Whelan, 1998; Smith, 1999). Importantly, *Escherichia coli* glycogen, with which the intracellular domain of fission yeast α -glucan synthase shares amino-acid sequence similarity (Hochstenbach *et al.*, 1998), requires a (1→4)- α -glucoooligosaccharide for chain initiation (Fox *et al.*, 1976; Kawaguchi *et al.*, 1978). Therefore, we speculate that the (1→4)-linked glucose residues found in fission-yeast α -glucan may form a primer molecule. However, it remained unclear whether the putative primer consists of consecutive (1→4)-linked glucose residues or whether it is composed of mixed (1→3)-linked and (1→4)-linked residues.

Here, we elucidate the chemical structure of the putative primer for fission-yeast α -glucan biosynthesis by digesting cell-wall α -glucan with an *endo*-(1→3)- α -glucanase preparation. To elucidate the chemical structure of the digestion products, an analysis strategy is developed that is based on a method described by Angel *et al.* (1991), involving oxidation of the oligosaccharides by periodate followed by reduction and per-*O*-methylation, and mass spectrometric analysis. To discriminate between 3-substituted and 4-substituted reducing ends, reducing residues are derivatized with the fluorescent label 2-aminobenzamide (2-AB) prior to oxidation tandem. By sequencing the derivatized oligosaccharides using nano-electrospray tandem mass spectrometry (nanoES-MS²), we demonstrate that the putative primer consists of consecutive (1→4)-linked α -glucose residues.

Results

Analysis method

To unambiguously discriminate between oligosaccharides containing (1→3)-linked and those containing (1→4)-linked hexoses, we developed a structural analysis method based on differences in chemical reactivity of these two types of linkage to periodate, which will oxidize residues with adjacent hydroxyl groups but will not affect other residues (Abdel-Akher *et al.*, 1952). In the case of →3)-Glc_p-(1→ and →4)-Glc_p-(1→ residues, only the latter will be oxidized, forming a polyaldehyde. This polyaldehyde is then reduced using sodium borodeuteride and per-*O*-methylated, resulting in a nominal mass of 208 amu, which is an increase of 4 atomic mass units (amu) per residue compared to →3)-Glc_p-(1→ residues treated the same way (Fig. 1). To identify the type of linkage of the reducing end, oligosaccharides are derivatized prior to oxidation using the fluorescent label 2-aminobenzamide (2-AB). Upon oxidation, the label cleaves off in case of 4-substitution, whereas it remains linked to the oligosaccharide when 3-substituted (Fig. 1). According to the reaction schemes shown in Fig. 1, the nominal mass of an oxidized/reduced, and methylated →3)-Glc_p-(1→[2AB] residue is 310 amu, whereas that of a →4)-Glc_p-(1→[2AB] residue is 121 amu. Similarly, a Glc_p-(1→ residue has a nominal mass of 179 amu. Thus, by measuring the molecular masses of oligosaccharides derived from (1→3)- α -glucanase-digested fission-yeast α -glucan following the structural analysis method, it is possible to

determine the number of (1→3)-linked and (1→4)-linked glucose residues plus the type of glycosidic linkage of the reducing end, and by selecting ions for collision-induced dissociation (CID), information on the sequence can be obtained.

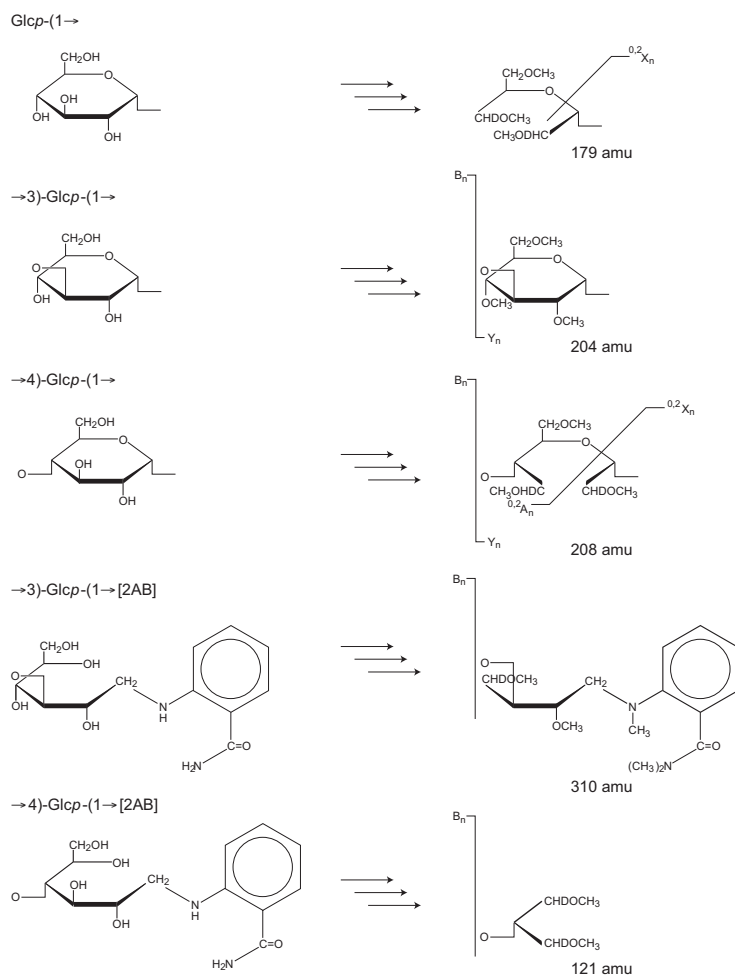


Fig. 1. Reaction scheme of periodate oxidation, reduction, and per-*O*-methylation on 3-substituted and 4-substituted glucose residues. Nominal masses of the reaction products are displayed next to theoretical fragmentation following the nomenclature of Domon and Costello (1988).

As model components to study our structural analysis method, we used laminaritetraose ((1→3)-β-glucotetraose) and maltotetraose ((1→4)-α-glucotetraose). Electrospray mass spectrometric analysis of the 2-AB-labeled and per-*O*-methylated laminaritetraose gave an ion at m/z 1047, representing a sodium-cationized, fully methylated tetrasaccharide that was derivatized at its reducing end (not shown). The nanoES mass spectrum of 2-AB-labeled laminaritetraose after periodate oxidation,

reduction, and per-*O*-methylation showed a sodium-cationized ion at m/z 920 (not shown). Combining the theoretical masses of the different constituents with the measured m/z value, we surmise that the ion is composed of one Glcp-(1→ (179 amu), two →3)-Glcp-(1→ (2 × 204 amu), one →3)-Glcp-(1→[2AB] (310 amu), and a sodium ion (23 amu), giving a total of 920 amu. To determine its sequence, we selected this ion for collision-induced dissociation. The nanoES tandem mass spectrum showed a range of fragment ions that according to the nomenclature formulated by Domon and Costello (1988), corresponded mainly to B-type and Y-type ions (Fig. 2). The ion at m/z 799 corresponded to an $^{0,2}X_3$ ion, representing 'cross-ring fragmentation' of the non-reducing residue. The spectrum contained a series of Y_n (m/z 742, 538, and 334), B_n (m/z 609), and C_n ions (m/z 423 and 627), arising from the cleavage of each successive glycosidic linkage. The fragmentation scheme demonstrated that each intrachain residue was substituted at C-3 (Fig. 2). Furthermore, the mass spectrum showed that the 2-AB label remains attached, indicating that the reducing end was 3-substituted.

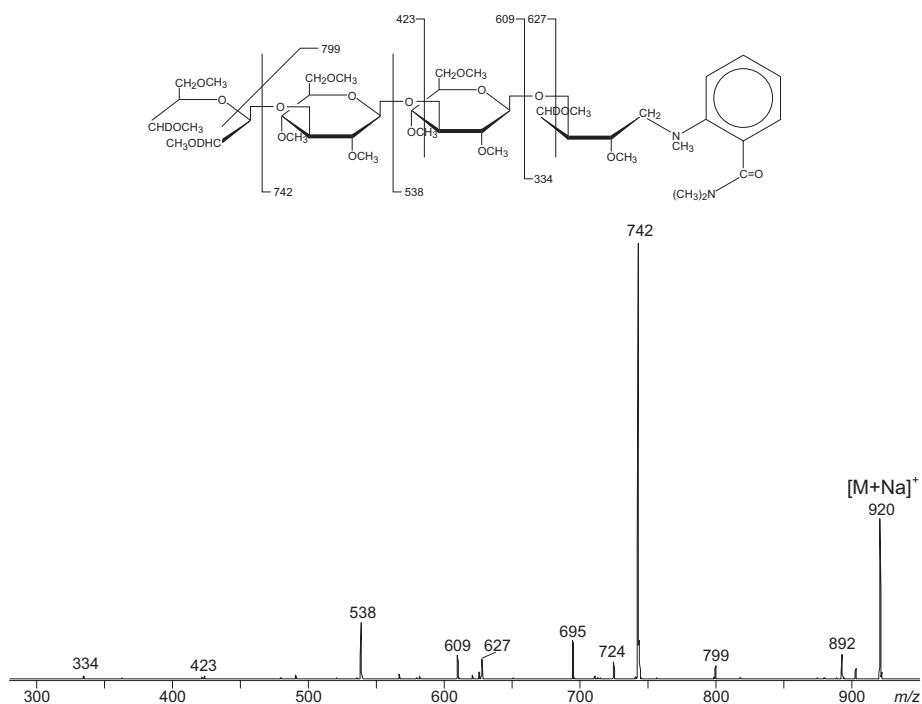


Fig. 2. Positive ion mode nanoES CID tandem mass spectrum of 2-AB labeled, periodate oxidized, and per-*O*-methylated laminaritetraose.

The nanoES mass spectrum of 2-AB-labeled, per-*O*-methylated maltotetraose showed an ion of high abundance at m/z 1047 that represented the fully-methylated compound (not shown). The 2-AB-labeled tetrasaccharide after oxidation, reduction, and per-*O*-methylation gave an ion at m/z 739, which corresponded to one Glcp-(1→ (179 amu), two

\rightarrow 4)-Glc_p-(1 \rightarrow) (208 amu each), one 4)-Glc_p-(1 \rightarrow [2AB] (121 amu) plus sodium. The nanoES tandem mass spectrum of the precursor ion at m/z 739 contained a series of Y_n and B_n ions at m/z 561, 353 and m/z 409, 617, respectively, arising from cleavage of each successive glycosidic linkage, as shown in the fragmentation scheme (Fig. 3). The fragmentation pattern showed that each intrachain residue had a nominal mass of 208 Da, representing oxidized (1 \rightarrow 4)-linked glucose residues. In addition, $^{0,2}X_n$ ions at m/z 618 and 410 and $^{0,2}A_n$ ions at m/z 352 and 560 were observed that confirmed the proposed structure. As shown in the fragmentation scheme of Fig. 3, the oxidation of 4-substituted reducing ends resulted in the release of the 2-AB label, and therefore, could clearly be distinguished from 3-substituted reducing ends (compare Fig. 3 with Fig. 2).

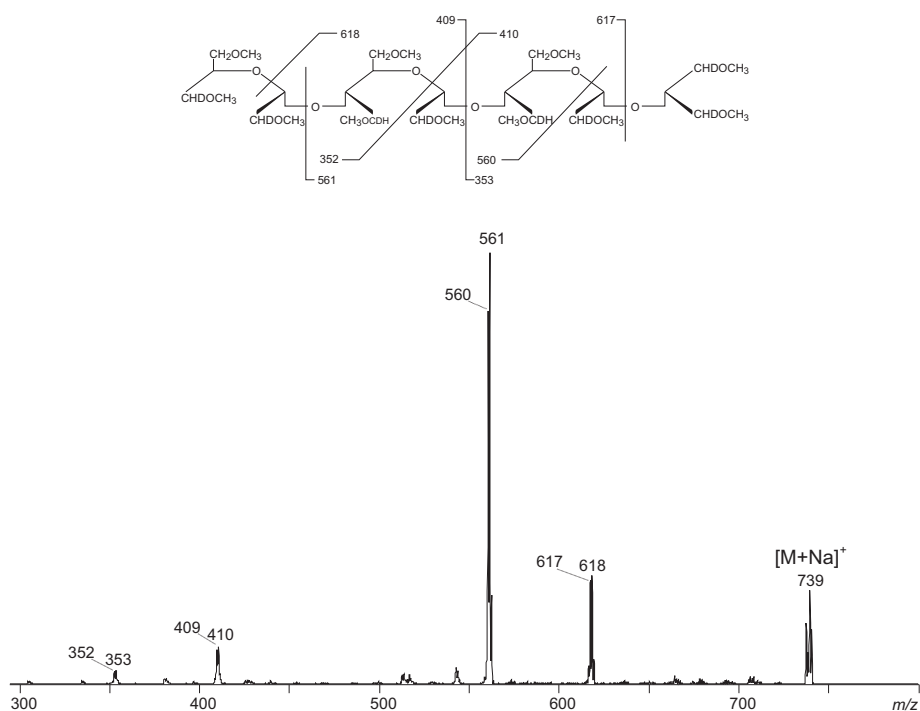


Fig. 3. Positive ion mode nanoES CID tandem mass spectrum of 2-AB labeled, periodate oxidized, and per-*O*-methylated maltotetraose.

Isolation and analysis of oligosaccharides derived from (1 \rightarrow 3)- α -glucanase digestion

To elucidate the primary structure of cell-wall α -glucan from fission yeast (wild-type strain FH023), we digested 100 mg of α -glucan using a (1 \rightarrow 3)- α -glucanase preparation. This glucanase has been isolated from a commercially available enzyme preparation of *Trichoderma harzianum*. It was shown that the enzyme has *endo*-catalytic activity and uses nigerotetraose as substrate to form nigerotriose and glucose (see Supplementary data at the end of this chapter). After desalting on Carboglyph solid phase extraction columns,

which in addition to desalting also removed monosaccharides, digestion products were fractionated on a Bio-Gel P4 column (Fig 4). Fractions 3 to 7 were further purified using high-performance anion-exchange chromatography (HPAEC) (Fig. 5).

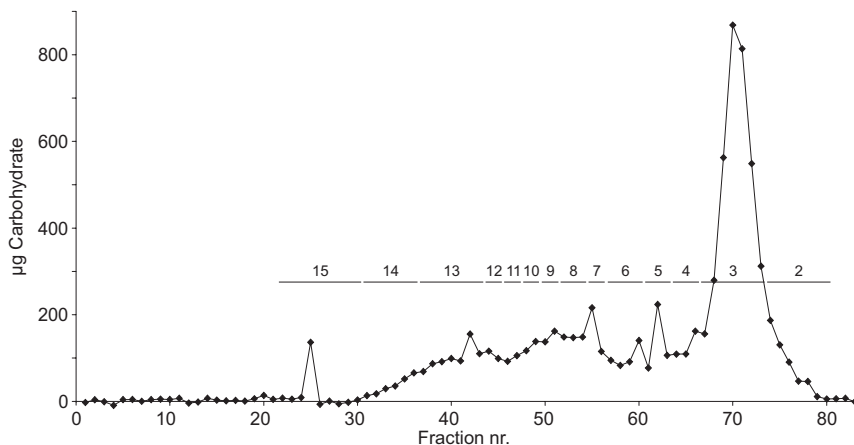


Fig. 4. Bio-Gel P4 size-exclusion chromatogram of *endo*-(1→3)- α -glucanase hydrolysis products of α -glucan from fission-yeast cell walls. Numbers indicate pooled fractions.

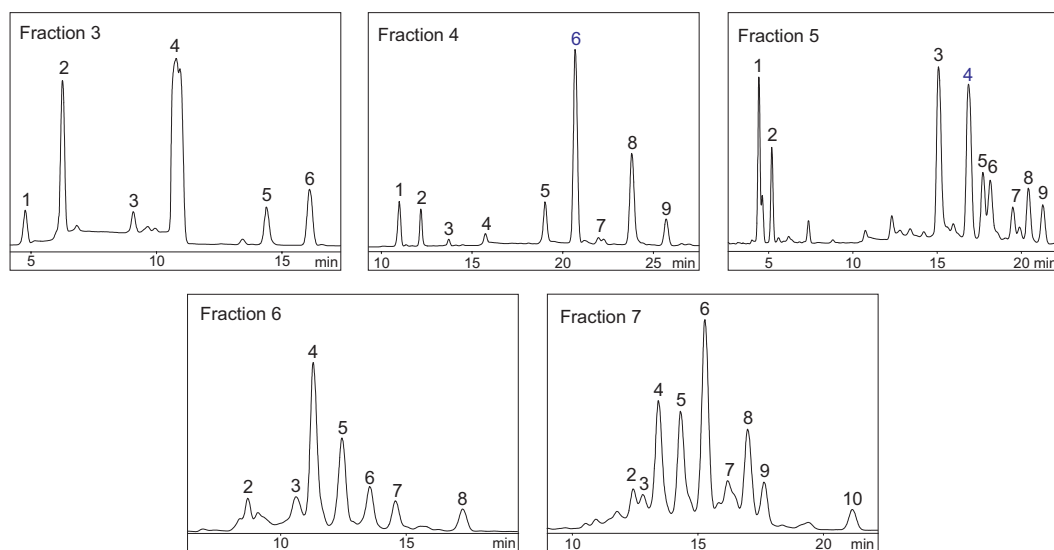
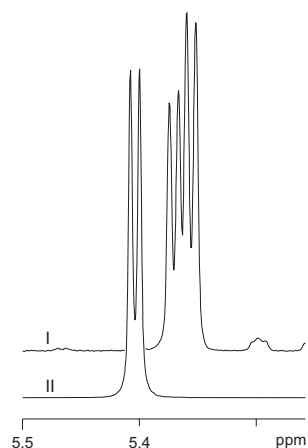


Fig. 5. Anion-exchange chromatograms of Bio-Gel P4 fractions 3-7 on a CarboPac PA1 column.

The HPAEC fractions were screened by $^1\text{H-NMR}$ spectroscopy for the presence of (1→3)-linked and (1→4)-linked α -Glc_p residues. The anomeric protons of (1→3)-linked α -glucopyranose residues have chemical shifts around 5.36 ppm (Fig. 6, spectrum I), whereas the anomeric protons of (1→4)-linked residues are found around 5.40 ppm

(Fig. 6, spectrum II), allowing rapid identification of the types of linkages. Fractions that contained (1→4)-linked glucose residues were then derivatized at their reducing end with 2-AB. One part was directly per-*O*-methylated in order to determine its molecular mass, whereas another part underwent the oxidation procedure of periodate oxidation, reduction, and per-*O*-methylation prior to analysis by nanoES mass spectrometry.

Fig. 6. Anomeric regions in the $^1\text{H-NMR}$ spectrum of nigerose (I) and maltose (II). Note that the anomeric proton of Glcp-(1→ in nigerose forms two doublets, which is due to the anomerization effect.



Fraction 3 — The HPAEC profile of fraction 3 showed six peaks of which subfraction 3.5 contained both (1→3)-linked and (1→4)-linked α -glucopyranose residues according to its $^1\text{H-NMR}$ spectrum (Fig. 7A). The mass spectrum of fraction 3.5 after 2-AB labeling and per-*O*-methylation showed an ion of high abundance at m/z 1047 representing fully per-*O*-methylated Hex₄ (not shown). In addition, an ion of low abundance was observed at m/z 843, representing fully per-*O*-methylated Hex₃, indicating a heterogeneous HPAEC fraction due to incomplete peak resolution for the oligosaccharides. After periodate oxidation, the mass of Hex₄ shifted to m/z 924 and hence may be composed of one Glcp-(1→, one →4)-Glcp-(1→, one →3)-Glcp-(1→, and one 3)-Glcp-(1→[2AB]. The nanoES tandem mass spectrum of precursor ion m/z 924 showed a range of fragment ions, of which Y₃ (m/z 746), Y₂ (m/z 538), and Y₁ (m/z 334) gave the full sequence of the tetrasaccharide as shown in the fragmentation scheme of Fig. 7B. The Y₁ ion clearly shows that the 2-AB label is still attached to the reducing end, demonstrating that the reducing residue is 3-substituted. According to the fragment ions, we conclude that the tetrasaccharide is Glcp-(1→4)-Glcp-(1→3)-Glcp-(1→3)-Glcp (Table I).

Fraction 4 — Fractionation of fraction 4 by HPAEC gave nine peaks that were analyzed by $^1\text{H-NMR}$ spectroscopy. Fractions 4.5 and 4.8 contained both (1→3)-linked and (1→4)-linked glucose residues, and were further analyzed by nanoES-MS. Analysis of fraction 4.5 by NMR spectroscopy and nanoES mass spectrometry showed that the major component is identical to that in fraction 3.5 (Fig. 8), which can be explained by incomplete separation of fractions 3 and 4 by Bio-Gel P4 size-exclusion chromatography.

The $^1\text{H-NMR}$ spectrum of fraction 4.8 showed anomeric signals of (1→4)-linked and (1→3)-linked Glcp (Fig. 9A). The mass spectrum of fraction 4.8 after 2-AB labeling and per-*O*-methylation showed predominantly two sodium-cationized pseudomolecular ions, an ion of high intensity at m/z 1251 that corresponds to a pentasaccharide and a low-intensity ion at m/z 1047 corresponding to a tetrasaccharide (not shown). Periodate oxidation followed by per-*O*-methylation gave a mass spectrum with ions at m/z 1128 and 1114, the latter indicating undermethylation (not shown). These m/z values showed that

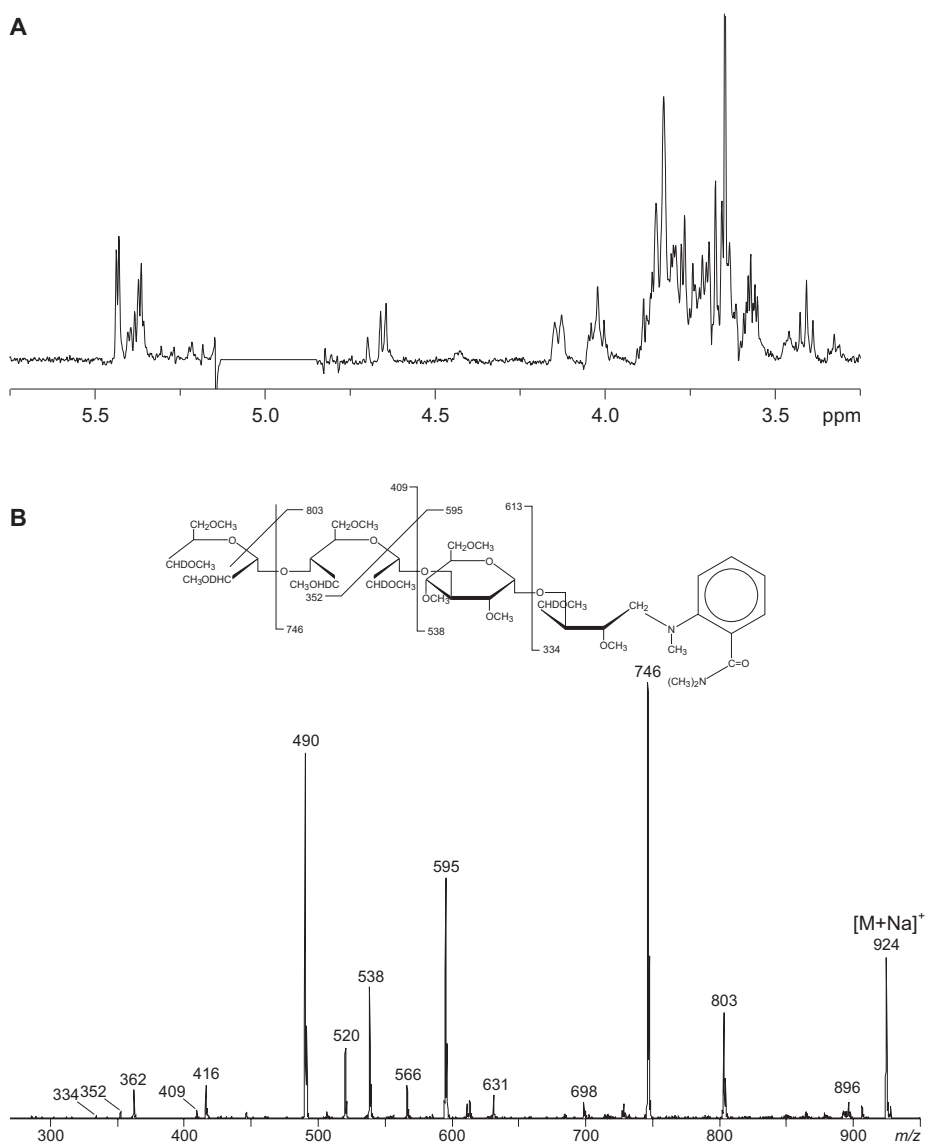


Fig. 7. Fraction 3.5 contains a tetrasaccharide with mixed (1→3)-linked and (1→4)-linked glucose residues. $^1\text{H-NMR}$ spectroscopy of HPAEC fraction 3.5 (**A**) and positive ion mode nanoES CID tandem mass spectrum of 2-AB labeled, periodate oxidized, and per-*O*-methylated HPAEC fraction 3.5, m/z 924.

fraction 4.8 contained a pentasaccharide composed of one *Glc*p-(1→, one →4)-*Glc*p-(1→, two →3)-*Glc*p-(1→, and one 3)-*Glc*p-(1→[2AB]. In the nanoES tandem mass spectrum of the sodium-cationized precursor ion at m/z 1128, Y_n^- , B_n^- , and $^{1,2}X_n^-$ -type ions were observed that gave the complete sequence of m/z 1128, namely *Glc*p-(1→4)-*Glc*p-(1→3)-*Glc*p-(1→3)-*Glc*p-(1→3)-*Glc*p (see fragmentation scheme in **Fig. 9B**, **Table I**).

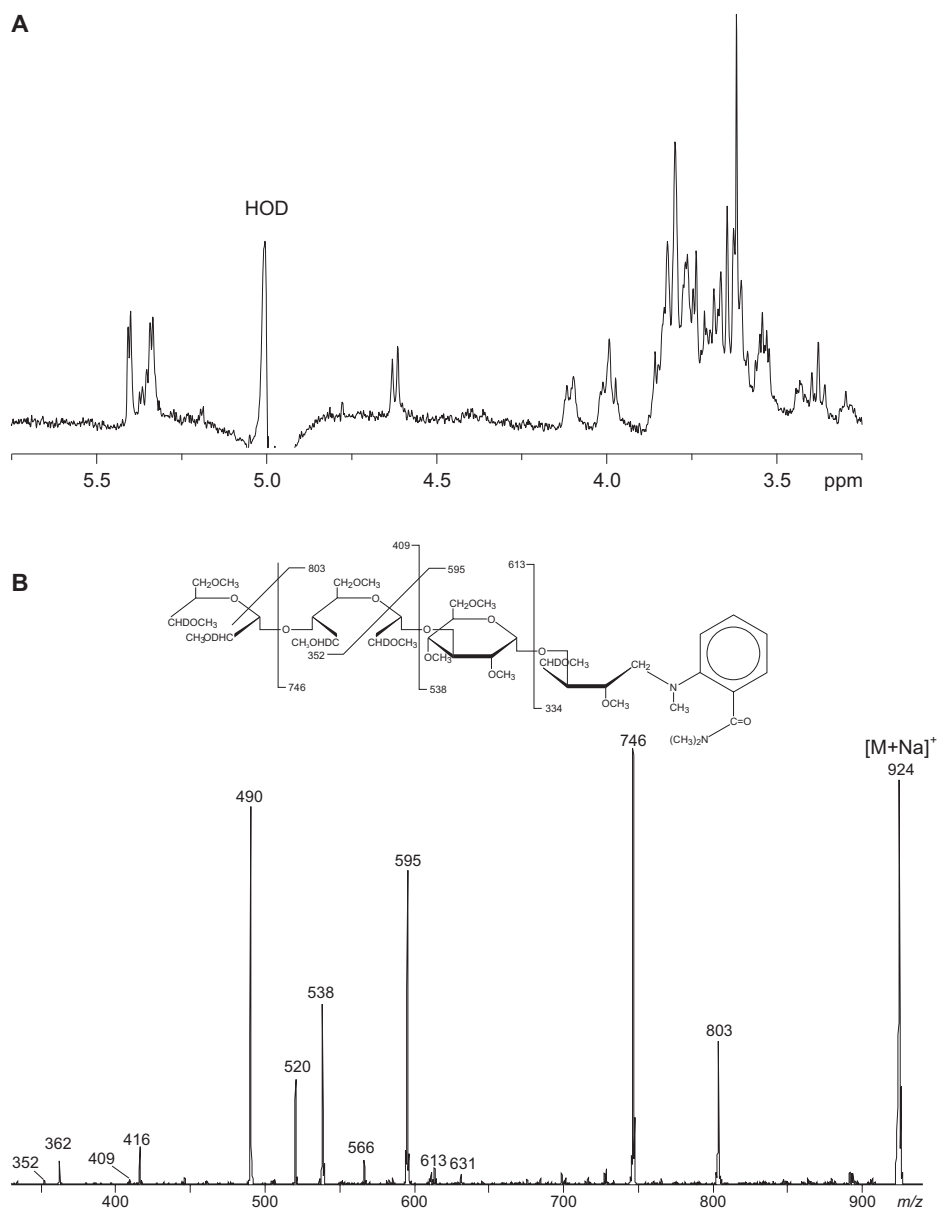


Fig. 8. Fraction 4.5 contains a tetrasaccharide with mixed (1→3)-linked and (1→4)-linked glucose residues. $^1\text{H-NMR}$ spectroscopy of HPAEC fraction 4.5 (A) and positive ion mode nanoES CID tandem mass spectrum of 2-AB labeled, periodate oxidized, and per-*O*-methylated HPAEC fraction 4.5, m/z 924 (B).

Fraction 5 — The fractionation of Bio-Gel P4 fraction 5 by HPAEC gave nine subfractions (Fig. 5). Of these fractions, $^1\text{H-NMR}$ spectroscopy indicated that fractions 5.3, 5.5, 5.6, and 5.8, are composed of (1→4)-linked *Glc*_p residues in addition to (1→3)-linked residues (Fig. 10-12). The mass spectrum obtained from the 2-AB labeled and per-*O*-methylated

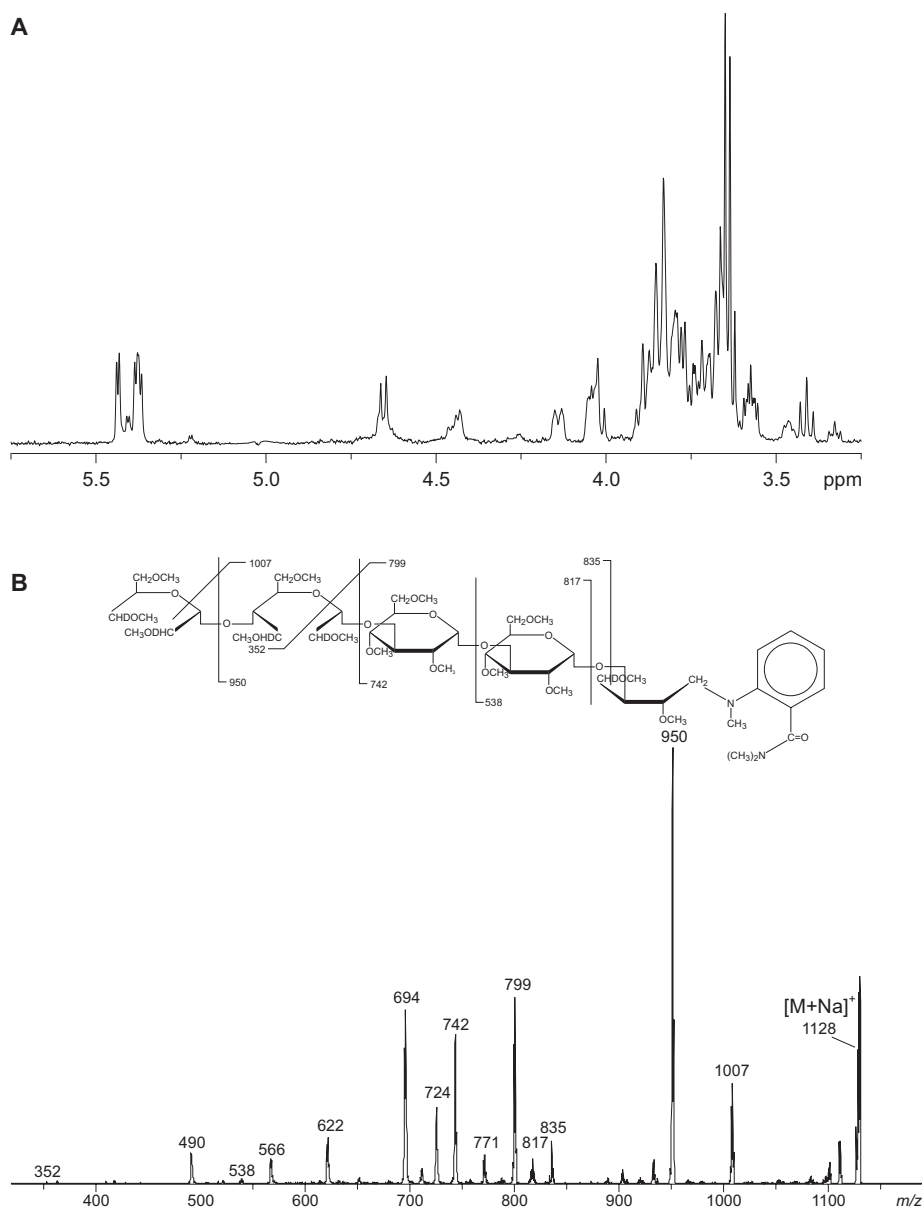


Fig. 9. Fraction 4.8 contains a pentasaccharide with mixed (1→3)-linked and (1→4)-linked glucose residues. $^1\text{H-NMR}$ spectroscopy of HPAEC fraction 4.8 (A) and positive ion mode nanoES CID tandem mass spectrum of 2-AB labeled, periodate oxidized, and per-O-methylated HPAEC fraction 4.8, m/z 1128 (B). Note that when selecting m/z 1128 for MS^2 , ratios between the isotopes of the pseudomolecular ion differed from natural abundance.

fraction 5.3 showed a major signal at m/z 1251, representing a fully methylated Hex₅. After applying the oxidation procedure, the mass spectrum showed an ion at m/z 1128,

The $^1\text{H-NMR}$ spectrum of fraction 5.5 indicated the presence of (1→4)-linked Glcp residues in addition to a small amount of (1→3)-linked residues (Fig. 11A). Mass-spectrometric analysis of per-*O*-methylated fraction 5.5 gave a low-intensity signal at m/z 1251, a medium-intensity signal at m/z 1455 and a signal of high intensity at m/z 1659, showing the presence of a mixture of sodium-cationized, fully-methylated penta-, hexa-, and heptasaccharides, respectively (not shown). The mass spectrum after applying the oxidation procedure showed a range of ions at m/z 986, 990, 1194, 1198, 1534, and 1548, of which the ion at m/z 1534 indicates undermethylation. Each of the ions was subsequently selected for collision-induced dissociation. In an effort to find the theoretical composition of the ion at m/z 990 according to the scheme in Fig. 1, we noticed that in the best fit (i.e., a pentasaccharide with (1→4)-linked residues, only), a mass difference of 43 amu occurred (namely m/z 990 vs. m/z 947), indicating underoxidation, which occurs when not all vicinal hydroxyl groups are oxidized. The tandem mass spectrum of the precursor ion at m/z 990 showed complete series of Y_n^- , B_n^- , and $^{1,2}X_n^-$ -type ions, giving the full sequence of the pentasaccharide (Fig. 11B). The fragmentation pattern showed the loss of the 2-AB group from the reducing end after periodate oxidation, demonstrating a 4-substituted reducing end. A B_4 ion was identified at m/z 825, indicating that the underoxidation occurred at the reducing end (Fig. 11B). According to the fragmentation, we conclude that fraction 5.5 contained Glcp-(1→4)-Glcp-(1→4)-Glcp-(1→4)-Glcp-(1→4)-Glcp (Table I), which is in accordance with the NMR data.

Table I. *endo*-(1→3)- α -glucanase treatment of α -glucan from fission-yeast cell walls

HPAEC fraction	m/z ¹ after per- <i>O</i> -methylation	m/z ¹ after oxidation	Structure ²	Origin
3.5	1047	924	○●●○	Center
4.5	1047	924	○●●○	Center
4.8	1251	1128	○●●○	Center
5.3	1251	1128	○●●○	Center
5.5	1251	990	○●●●	Reducing end
	1455	1198	○●●●	Reducing end
	1659	1548	○●●●	Center
5.6	1455	1198	○●●●	Reducing end
5.8	1659	1406	○●●●	Reducing end
6.3	1455	1198	○●●●	Reducing end
	1659			
6.4	1659	1198, 1402	○●●●	Reducing end
	1863	1742	○●●●	Center
6.7	1455	1402	○●●●	Reducing end
7.5	1455, 1659, 1863	1818	○●●●	Reducing end

¹ m/z ratios correspond to $[M + Na]^+$ ions.

² White spheres: non-reducing end; black spheres: (1→4)-linked residues; grey spheres: (1→3)-linked residues; reducing ends are marked with a diagonal line.

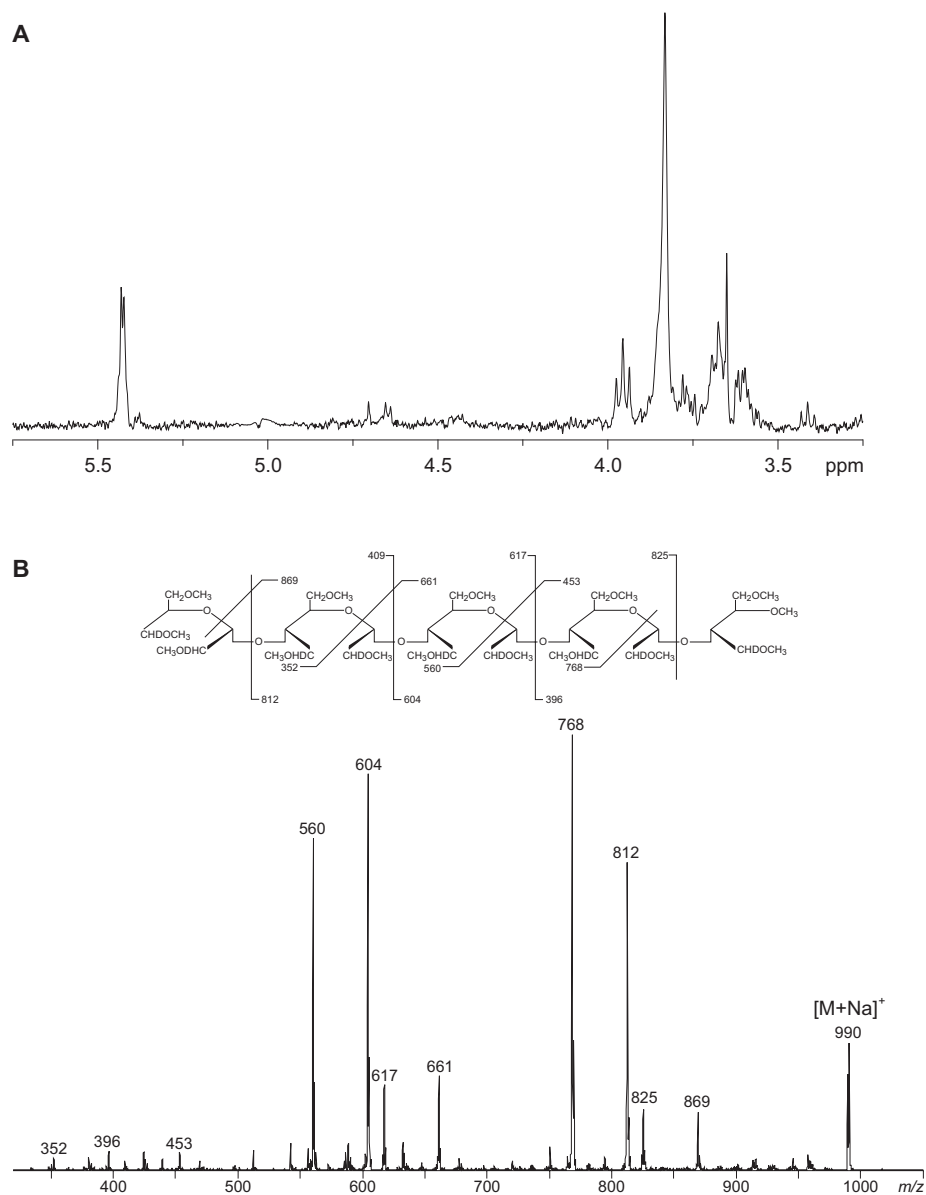
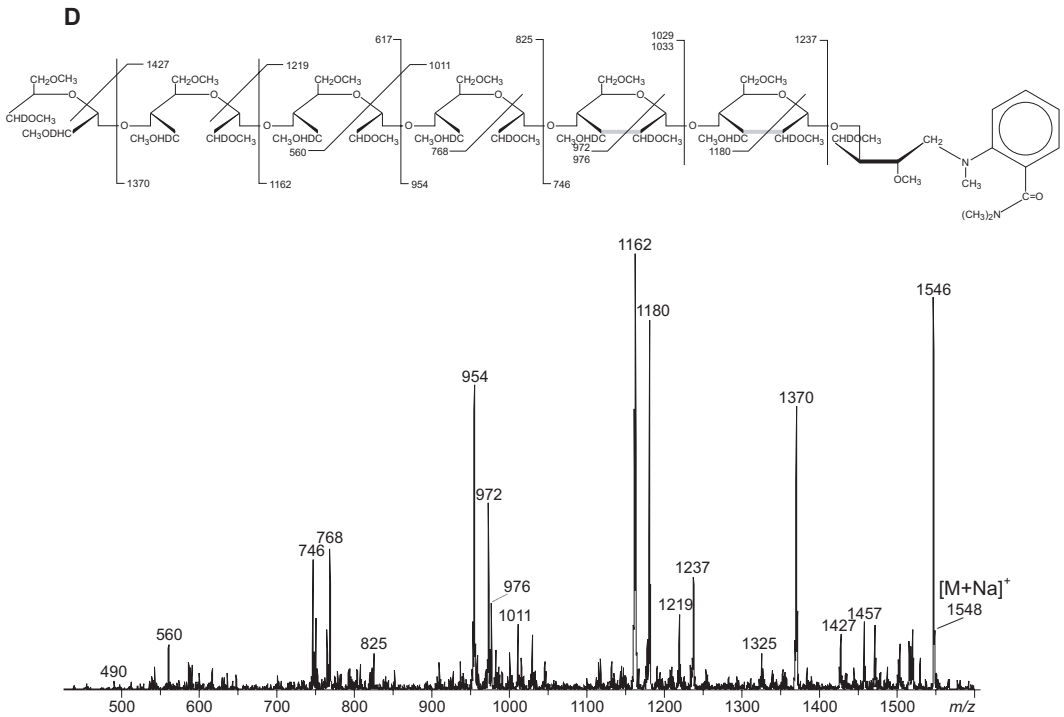
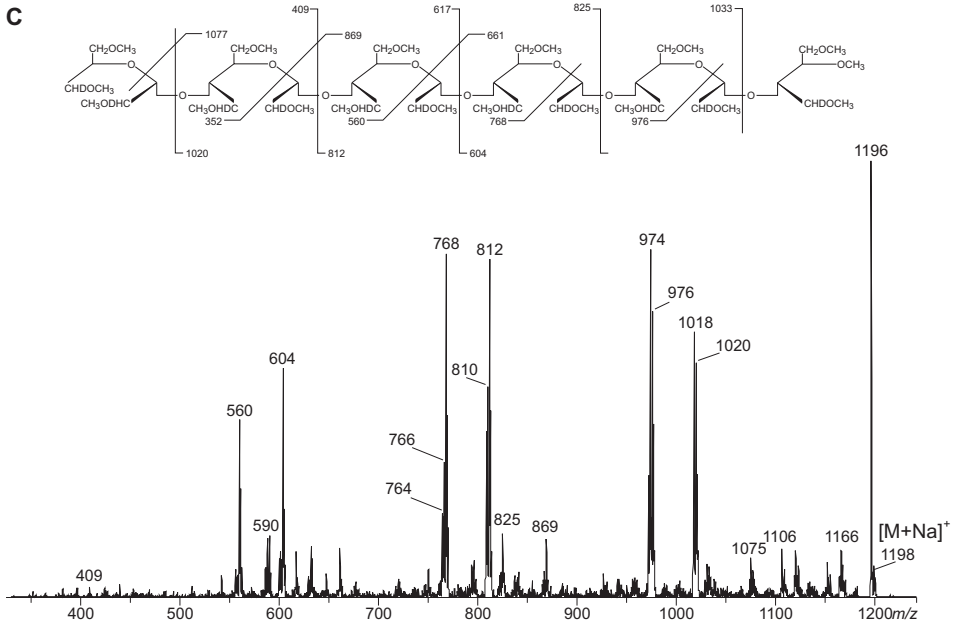


Fig. 11. Fraction 5.5 comprises a mixture of oligosaccharides. $^1\text{H-NMR}$ spectroscopy of HPAEC fraction 5.5 (A) and positive ion mode nanoES CID tandem mass spectrum of 2-AB labeled, periodate oxidized, and per-*O*-methylated HPAEC fraction 5.5, m/z 990 (B), m/z 1198 (C), and m/z 1548 (D). Note that when selecting m/z 1198 for MS², besides the intended precursor ion, also isotopes of the m/z 1194 cluster were selected, resulting in a high-abundant ion at m/z 1196. This also explains the presence of fragment ions at m/z 1018, 974, 810, etc.



We then selected the ion at m/z 986 for collision-induced dissociation. Since this ion had a mass difference of 4 amu compared to the ion at m/z 990, it indicates the presence of either a (1→3)-linked residue, or underoxidation of a (1→4)-linked residue. In both cases a residue of 204 amu is found when analyzing the tandem mass spectrum. In the first case,

it is likely that the (1→3)-linked residue is present at a specific location, whereas under-oxidation may occur at virtually any residue. This was investigated by selecting the ion at m/z 986 for tandem mass spectrometric analysis, which gave a fragmentation pattern similar to that of the precursor ion at m/z 990, including 1,2A_2 , 1,2A_3 , 1,2A_4 , 1,2X_3 , 1,2X_4 , and 1,2X_5 ions, giving the complete sequence of (1→4)-linked residues (not shown) indicating that underoxidation is more likely than the presence of an additional (1→3)-linked residue.

The next ion observed in the nanoES mass spectrum, at m/z 1198 was a hexasaccharide that may be composed entirely of (1→4)-linked glucose residues. The tandem mass spectrum of precursor ion m/z 1198 indeed showed that the hexasaccharide was composed of (1→4)-linked residues, only (**Fig. 11C**, **Table I**). Similar to the ion at m/z 990, this compound was also accompanied by an underoxidized form, observed at m/z 1194.

The ion at m/z 1548 was theoretically composed of one Glcp-(1→, four →4)-Glcp-(1→, one →3)-Glcp-(1→, and one →3)-Glcp-(1→[2AB]. The tandem mass spectrum (**Fig. 11D**) showed almost complete series of Y_n - and B_n -type fragment ions that, together with the presence of 1,2A_n - and 1,2X_n -type ions at m/z 560, 768, 976 and m/z 1427, 1219, 1011, respectively, gave the complete sequence of the ion at m/z 1548 (see fragmentation scheme in **Fig. 11D**). According to the fragmentation scheme, the 2-AB label is still attached to the oligosaccharide, indicating 3-substituted reducing end (**Table I**). There may be a second (1→3)-linked residue, although the presence of ions at m/z 1237, 1180, 1029, and 972 suggest underoxidation (indicated as grey lines in **Fig. 11D**).

The mass spectrum of fraction 5.6 after 2-AB labeling and per-*O*-methylation showed an ion of high abundance at m/z 1455, together with ions of low abundances at m/z 1251 and m/z 1659, corresponding to sodium cationized pseudomolecular Hex₆, Hex₅, and Hex₇, respectively (not shown). The nanoES mass spectrum of fraction 5.6 after periodate oxidation showed predominantly an ion at m/z 1198 (not shown), and therefore, the fraction contained a hexasaccharide composed entirely of (1→4)-linked Glcp residues (**Table I**).

The last fraction in this series, fraction 5.8, predominantly consisted of (1→4)-linked Glcp residues as determined by 1H -NMR spectroscopy (**Fig. 12A**); (1→3)-linked residues were not detected. The mass spectrum showed an ion of high abundance at m/z 1659 next to an ion of low abundance at m/z 1455, analogous to sodium-cationized, fully per-*O*-methylated and 2-AB-derivatized Hex₇ and Hex₆, respectively (not shown). After applying the oxidation procedure, ions at m/z 1402, 1406, 1194, and 1198 were observed in the nanoES mass spectrum. Since the ions at m/z 1402 and 1194 presumably originated from underoxidation, we focused on the structures of the other ions. The mass of the pseudomolecular ion at m/z 1406 suggested that the main component in fraction 5.8 was a heptasaccharide composed of (1→4)-linked Glcp residues, only (**Table I**). This was confirmed by the nanoES tandem mass spectrometry (**Fig. 12B**) of the precursor ion at m/z 1406 that gave a fragmentation pattern corresponding with Glcp-(1→4)-Glcp-(1→4)-Glcp-(1→4)-Glcp-(1→4)-Glcp-(1→4)-Glcp-(1→4)-Glcp.

The ion at m/z 1198 differed 208 amu from the ion at m/z 1406, and therefore, must be a 2-AB-derivatized, oxidized, and fully per-*O*-methylated hexasaccharide consisting of (1→4)-linked glucose residues. These results show that fraction 5.8 contained two components, namely a heptasaccharide and a hexasaccharide that both are composed entirely of (1→4)-linked α -Glc_p residues.

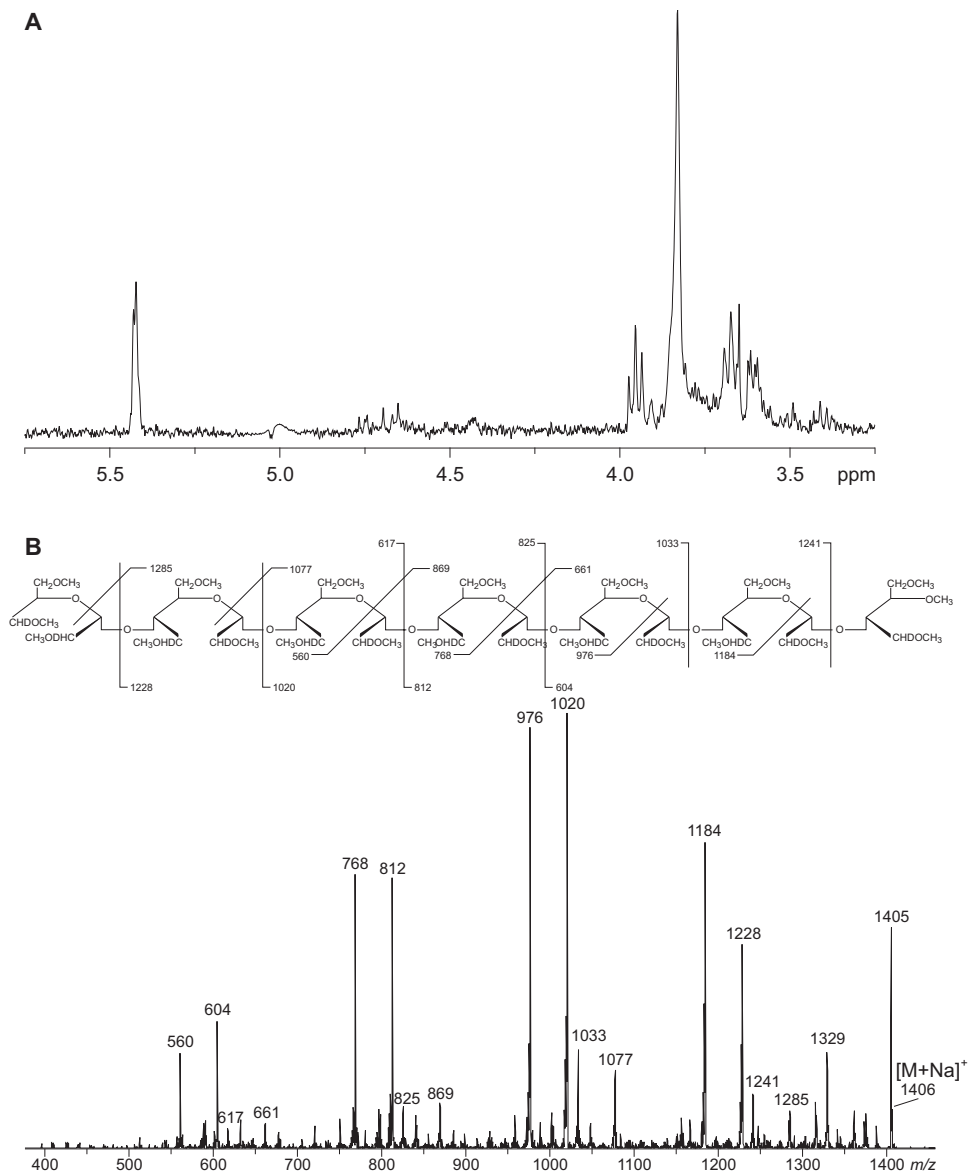


Fig. 12. Fraction 5.8 contains a heptasaccharide consisting of (1→4)-linked glucose residues. ^1H -NMR spectroscopy of HPAEC fraction 5.8 (A) and positive ion mode nanoES CID tandem mass spectrum of 2-AB labeled, periodate oxidized, and per-*O*-methylated HPAEC fraction 5.8, m/z 1406 (B).

Fraction 6 — Fractioning Bio-Gel P4 fraction 6 by HPAEC gave approximately eight well resolved peaks (Fig. 5), of which fractions 6.3, 6.4, and 6.7 were analyzed further by nanoES-MS. The $^1\text{H-NMR}$ spectrum of fraction 6.3 showed two anomeric signals corresponding to (1 \rightarrow 4)-linked and (1 \rightarrow 3)-linked Glcp residues (Fig. 13A). The nanoES

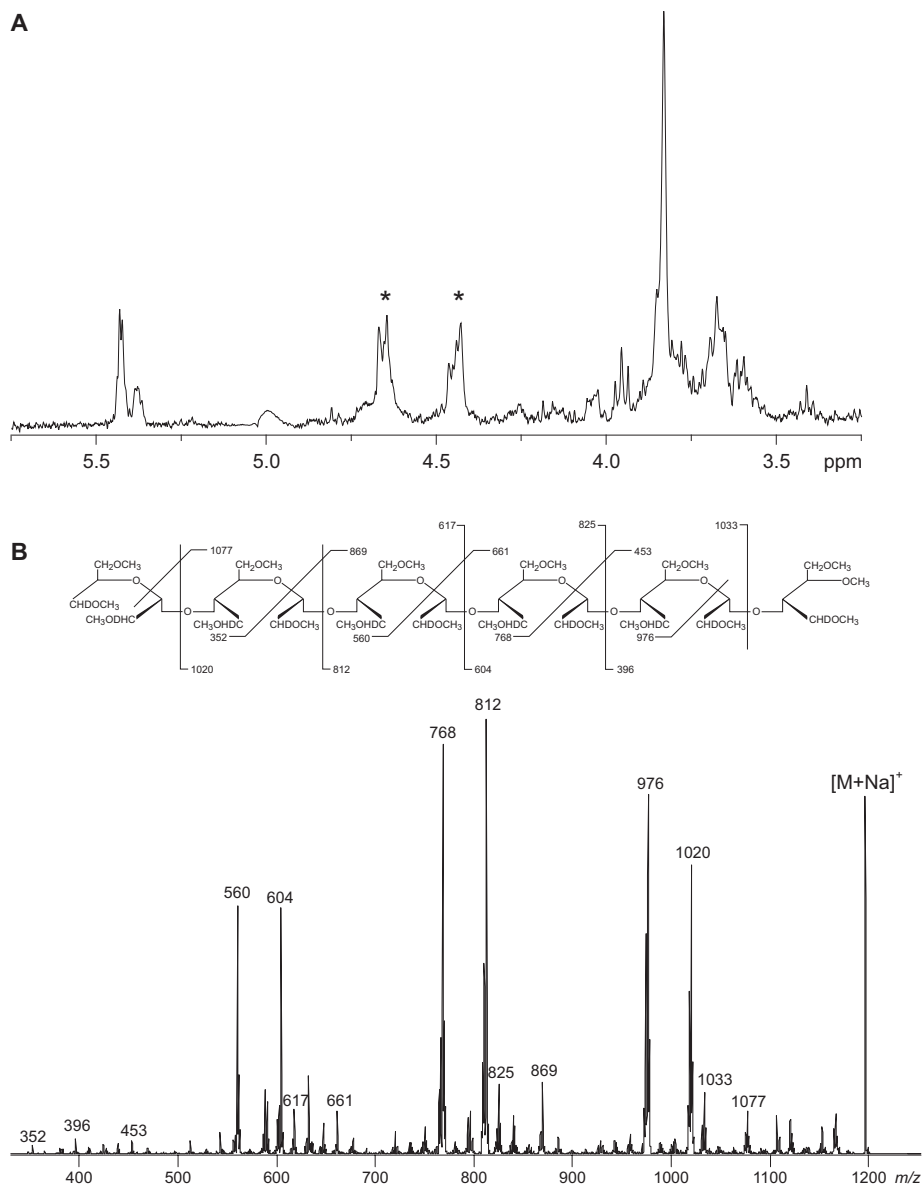


Fig. 13. Fraction 6.3 contains a hexasaccharide consisting of (1 \rightarrow 4)-linked glucose residues. $^1\text{H-NMR}$ spectroscopy of HPAEC fraction 6.3 (A) and positive ion mode nanoES CID tandem mass spectrum of 2-AB labeled, periodate oxidized, and per-*O*-methylated HPAEC fraction 6.3, m/z 1198 (B). NMR signals indicated with an asterisk (*) belong to an unknown contamination.

mass spectrum of the 2-AB labeled and per-*O*-methylated sample showed one signal of high abundance at m/z 1659, corresponding to a fully per-*O*-methylated heptasaccharide (not shown). In addition, a signal of medium abundance was detected at m/z 1455, which corresponded to a fully per-*O*-methylated hexasaccharide. The nanoES mass spectrum of fraction **6.3** after 2-AB labeling, oxidation/reduction and per-*O*-methylation gave two ions of high abundance at m/z 1194 and 1198, of which the latter corresponded to a hexasaccharide composed of (1→4)-linked glucose residues, only (not shown). This was confirmed by selecting the ion at m/z 1198 for tandem mass spectrometry (**Fig. 13B, Table I**). Tandem MS analysis of the ion at m/z 1194 showed that this ion originated from underoxidation (not shown). Importantly, a heptasaccharide was not identified, which is in contrast with the observations made for the MS analysis of the per-*O*-methylated sample, indicating that fraction **6.3** was slightly degraded due to overoxidation. Overoxidation is the degradation of 4-substituted reducing ends, that gradually processes towards the non-reducing end by hydrolyzing glycosidic linkages (Dyer, 1956). An erroneous calculation of the degree of polymerization can be the result, but by comparing the molecular masses before and after oxidation, overoxidation is readily noticed.

The $^1\text{H-NMR}$ spectrum of fraction **6.4** showed an anomeric signal corresponding to (1→4)-linked *Glc*_p residues (**Fig. 14A**). MS analysis after 2-AB labeling and per-*O*-methylation gave an ion of high abundance at m/z 1863 and a signal of medium abundance at m/z 1659, corresponding to an octasaccharide and a heptasaccharide, respectively (not shown). The nanoES mass spectrum of fraction **6.4** undergoing the oxidation procedure showed ions at m/z 1194, 1198, 1398, 1402, and 1742 (not shown). Of these, the ion at m/z 1198 corresponded to a hexasaccharide consisting of (1→4)-linked glucose residues, only (**Fig. 14B, Table I**), whereas the ion at m/z 1194 originated from underoxidation (not shown). Both ions were probably formed by overoxidation of a (1→4)-linked heptasaccharide. Similarly, tandem mass spectrometry showed that the ions at m/z 1398 and 1402 corresponded to singly and doubly underoxidized (1→4)-linked heptasaccharides, respectively. When selecting the ion at m/z 1742 for collision-induced dissociation, we obtained a mass spectrum that corresponded to an octasaccharide with the 2-AB label still attached to the octasaccharide, indicating a 3-substituted reducing end (**Fig. 14C, Table I**). According to the fragmentation scheme, multiple-underoxidation may have occurred, and therefore, we presume that the ion at m/z 1742 is derived from *Glc*_p-(1→4)-*Glc*_p-(1→4)-*Glc*_p-(1→4)-*Glc*_p-(1→4)-*Glc*_p-(1→4)-*Glc*_p-(1→4)-*Glc*_p-(1→3)-*Glc*_p.

The $^1\text{H-NMR}$ spectrum obtained from fraction **6.7** showed two anomeric signals, corresponding to (1→4)-linked and (1→3)-linked *Glc*_p residues (**Fig. 15A**). Analysis of this fraction after 2-AB labeling and per-*O*-methylation by nanoES-MS gave an ion at m/z 1455, indicating a fully methylated heptasaccharide (not shown). After periodate oxidation, reduction, and per-*O*-methylation, two ions were present in the mass spectrum at m/z 1398 and 1402 (not shown). The ion at m/z 1402 was selected for collision induced dissociation, which gave a fragmentation pattern consistent with a *Glc*_p-(1→3)-*Glc*_p-(1→4)-*Glc*_p-(1→4)-*Glc*_p-(1→4)-*Glc*_p-(1→4)-*Glc*_p (**Fig. 15B, Table I**).

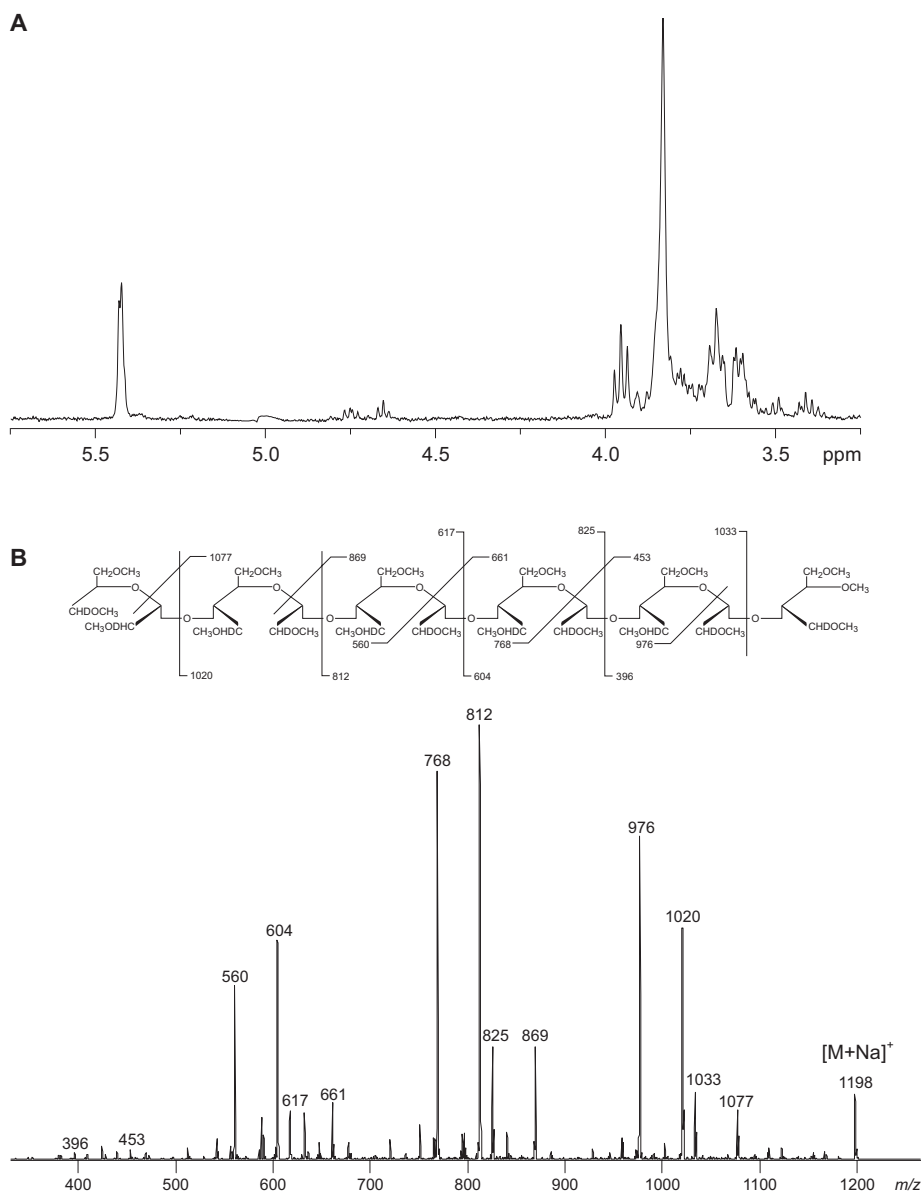
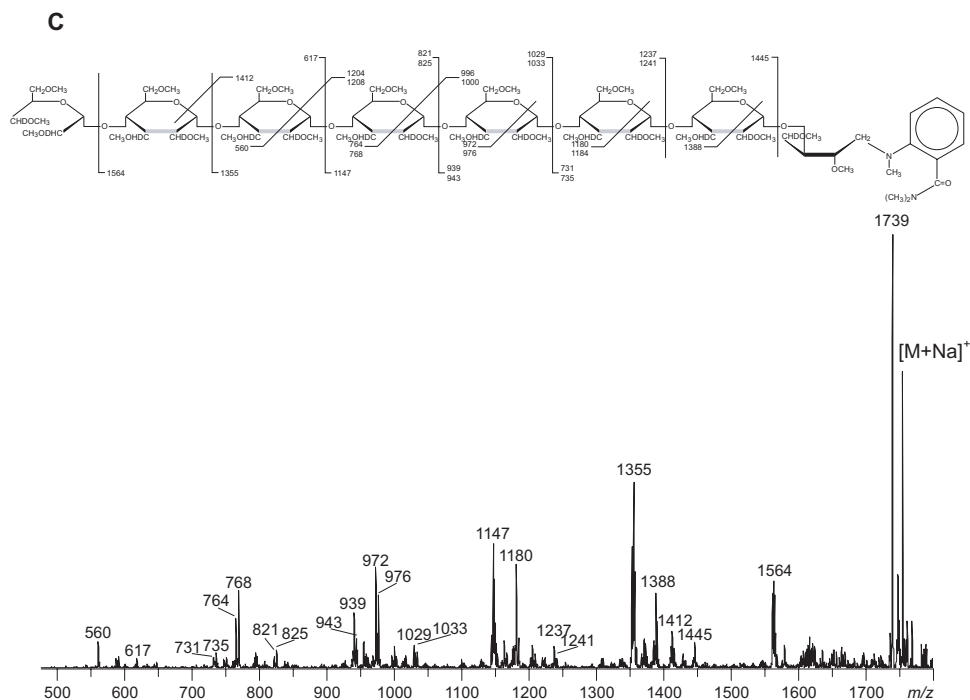


Fig. 14. Fraction 6.4 consists of a mixture of oligosaccharides. $^1\text{H-NMR}$ spectroscopy of HPAEC fraction 6.4 (A) and positive ion mode nanoES CID tandem mass spectrum of 2-AB labeled, periodate oxidized, and per-*O*-methylated HPAEC fraction 6.4, m/z 1198 (B) and m/z 1742 (C). Linkages indicated in grey indicate possible underoxidation between C-2 and C-3.

Fraction 7 — HPAEC fractionation of Bio-Gel P4 fraction 7 gave ten major fractions (Fig. 5), of which $^1\text{H-NMR}$ analysis showed that fraction 7.5 contains both (1 \rightarrow 4)-linked and (1 \rightarrow 3)-linked α -Glc_p (Fig. 16A). The positive ion mode ES mass spectrum obtained



from per-*O*-methylated fraction 7.5 was of poor quality showing ions at m/z 1455, 1659, and 1863, representing a sodium-cationized, 2-AB labeled, and fully per-*O*-methylated hexasaccharide, heptasaccharide, and octasaccharide, respectively (not shown). The ES mass spectrum of this fraction after applying the oxidation procedure, also was of poor quality (not shown). An ion was observed at m/z 1818 that according to its mass-to-charge ratio may be composed of a nonasaccharide containing one *Glc*p-(1→, six →4)-*Glc*p-(1→, and one 4)-*Glc*p residues plus one →3)-*Glc*p-(1→ residue or one underoxidation. The ES tandem mass spectrum of this ion gave the complete sequence of the nonasaccharide, clearly indicating that a single underoxidation occurred (**Fig. 16B**, possible positions of underoxidation indicated by a grey line). Therefore, the fragmentation indicates that the nonasaccharide may be composed of (1→4)-linked glucose residues, only (**Table I**).

Due to the poor quality of the mass spectrum of fraction 7.5, other ions than m/z 1818 could not be selected for collision-induced dissociation. Importantly, the nonasaccharide that we were able to identify by ES mass spectrometric analysis of the oxidized sample, was missing in the nanoES mass spectrum obtained from the per-*O*-methylated sample. This observation may be explained by the high mass-to-charge ratio of this ion, m/z 2076 for a single-charged pseudo-molecular ion, which exceeded the mass range of the mass spectrometer. Furthermore, $^1\text{H-NMR}$ spectrometry indicated the presence of some (1→3)-linkages. We assume that these residues were present as minor components that were overlooked, again due to the poor quality of the mass spectra.

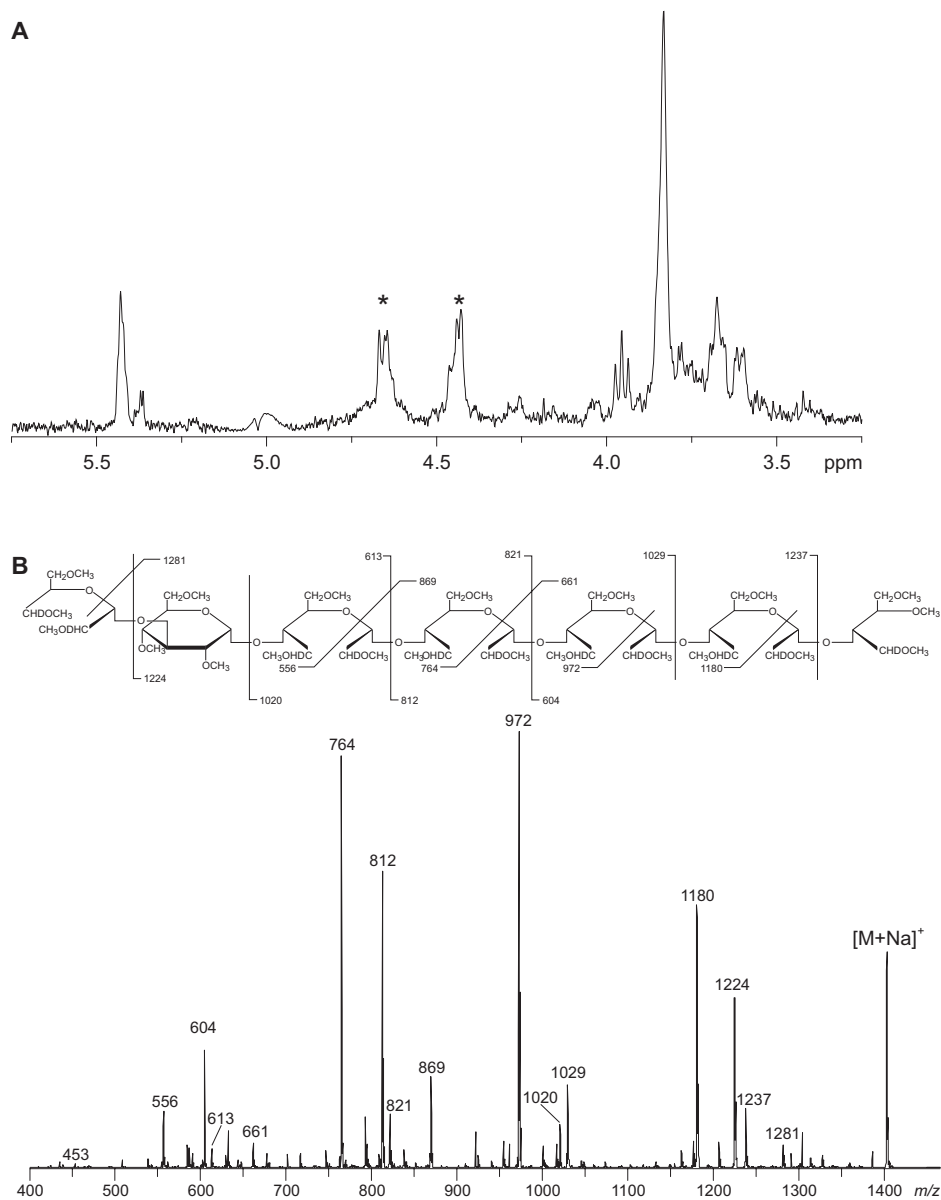


Fig. 15. Fraction 6.7 contains a heptasaccharide consisting of mixed (1→4)-linked and (1→3)-linked glucose residues. $^1\text{H-NMR}$ spectroscopy of HPAEC fraction 6.7 (A) and positive ion mode nanoES CID tandem mass spectrum of 2-AB labeled, periodate oxidized, and per-O-methylated HPAEC fraction 6.7, m/z 1402 (B). NMR signals indicated with an asterisk (*) belong to an unknown contamination.

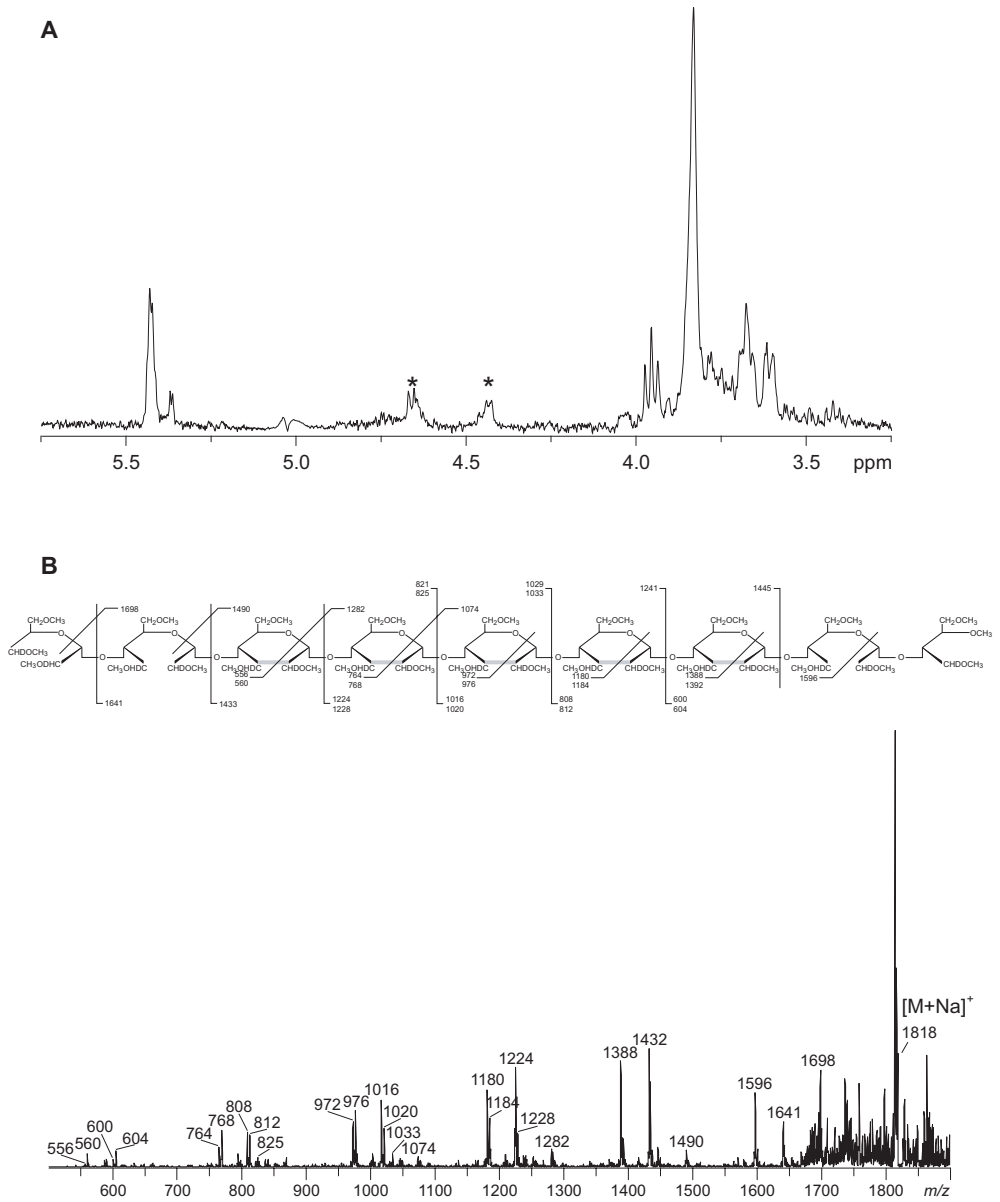


Fig. 16. Fraction 7.5 contains a nonasaccharide consisting of (1→4)-linked glucose residues. $^1\text{H-NMR}$ spectroscopy of HPAEC fraction 7.5 (**A**) and positive ion mode nanoES CID tandem mass spectrum of 2-AB labeled, periodate oxidized, and per-*O*-methylated HPAEC fraction 7.5, m/z 1818 (**B**). NMR signals indicated with an asterisk (*) belong to an unknown contamination. Linkages indicated in grey indicate possible underoxidation between C-2 and C-3.

Discussion

Fission-yeast α -glucan

Here, we have characterized the stretches containing (1 \rightarrow 4)-linked glucose residues present in cell-wall α -glucan of fission yeast after removing the (1 \rightarrow 3)-linked glucose residues by *endo*-(1 \rightarrow 3)- α -glucanase digestion. Analysis of the glucanase-resistant material showed that two classes of products were present. The first class comprises linear oligosaccharide structures composed of one or more consecutive (1 \rightarrow 4)-linked α -glucose residues linked to an oligomer of two or more, (1 \rightarrow 3)-linked glucose residues. Taking into consideration the catalytic mechanism of *T. harzianum* (see Supplemental data at the end of this chapter) together with our observation that fission-yeast α -glucan is resistant towards glucoamylase digestion (Chapter 2), we propose that this class of oligosaccharides originates from the intrachain region of α -glucan that links two (1 \rightarrow 3)- α -glucan segments via a number of (1 \rightarrow 4)-linked glucose residues (Fig. 17).

The second class consists of linear oligosaccharides that are composed exclusively of (1 \rightarrow 4)-linked α -Glc_p residues, or, in a single case, with a (1 \rightarrow 3)-linked non-reducing end. Taking into consideration the catalytic mechanism of the (1 \rightarrow 3)- α -glucanase preparation we assume that the second class of oligosaccharides was derived from the reducing end of the α -glucan polymer (Fig. 17). Previously, we showed that fission-yeast α -glucan is composed of two building blocks, each consisting of a (1 \rightarrow 3)- α -glucan segment with a short stretch containing (1 \rightarrow 4)-linked glucose residues. In the present study, we demonstrated that this stretch consists of oligomers of consecutive (1 \rightarrow 4)-linked glucose residues.

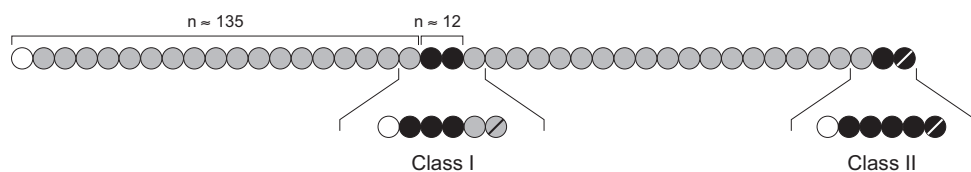


Fig. 17. Schematic representation of α -glucan from fission-yeast cell walls. Digestion of α -glucan with an *endo*-(1 \rightarrow 3)- α -glucanase gave two classes of oligosaccharides, depending on whether they originated from the center part of the α -glucan molecule (Class I) or from the reducing end (Class II). White spheres: non-reducing end; black spheres: (1 \rightarrow 4)-linked residues; grey spheres: (1 \rightarrow 3)-linked residues; reducing ends are marked with a diagonal line.

Sequencing structurally closely related oligosaccharides

Complete structural elucidation of oligosaccharides containing chemically similar linkages by NMR spectroscopy is not always possible due to strong overlapping of signals. Linkage analysis gives quantitative information on the type of linkages (Lindberg, 1972), but the lack of sequence information and the relative high amounts that are needed necessitates the use of other methods. Mass spectrometry of per-*O*-acetylated or per-*O*-

methylated oligosaccharides is a highly sensitive technique that can be used for complete structural characterization of oligosaccharides (Dell & Morris, 2001; Dell *et al.*, 1997; Costello, 1997), but often relies on the presence of specific cross-ring fragmentation and the absence of others such that unambiguous determination of glycosidic linkages is not always possible. Our structural analysis method allowed us to rapidly sequence structurally closely related oligosaccharides. The method is based on differences in reactivity towards periodate in combination with nanoES mass spectrometry. We showed that this method can be used to unambiguously differentiate between (1→3)-linked and (1→4)-linked hexose residues. By using collision-induced dissociation, we were able to determine the sequences of oligosaccharides. Importantly, this method can be extended readily to other types of linkages, linear as well as branched oligosaccharides, and *N*-glycans derived from glycoproteins. Limitations encountered in this method include under- and overoxidation. Misinterpretation may be the result of underoxidation because (1→4)-linked residue may than have the same nominal mass as (1→3)-linked residues. However, since underoxidation occurs virtually randomly, this will be noticed readily. Overoxidation, on the other hand, leads to degradation of 4-substituted oligosaccharides starting from the reducing end and processing towards the non-reducing end (Dyer, 1956). Thus, the result may be an erroneous determination of the degree of polymerization of the molecule. Nonetheless, by comparing molecular masses of oligosaccharides before and after applying the oxidation procedure, overoxidation can be noticed easily and corrections can be made concerning the proposed structures.

A second limitation was encountered with a decrease in detection sensitivity with increasing molecular mass, which is common to carbohydrates. In addition to strong heterogeneity of high-molecular mass fractions, we were unable to obtain decent mass spectra of oligosaccharides with a degree of polymerization higher than approximately eight. Therefore, we only analyzed the first seven out of fifteen Bio-Gel P4 fractions. Although only a limited number of fractions were analyzed, we consider these fractions to be representative structures of the (1→4)-linked stretch present in fission-yeast α -glucan.

Finally, for the hydrolysis of α -glucan, we used an *endo*-(1→3)- α -glucanase preparation that was purified by binding to its substrate (see Supplementary data at the end of this chapter). Despite this substrate-specific purification, we cannot exclude the possibility of co-purification of contaminating enzymes, such as amylases, and although we could not determine such enzyme activity, we hydrolyzed fission-yeast α -glucan during a number of short 1-h incubations to minimize the chance of degradation with contaminating enzymes.

Concluding remarks

α -Glucan is present in the cell walls of many fungi at levels varying from 9 to 46%, depending on the fungal species. The basic chemical compositions of α -glucans from a number of fungal species have been elucidated, and interestingly, many α -glucans are

composed similar to that of fission yeast. For instance, α -glucans from *Aspergillus* species, *Fusicoccum amygdali*, *Neurospora crassa*, and *Cryptococcus neoformans*, like fission-yeast α -glucan, consist mainly of (1 \rightarrow 3)-linked α -Glc_p residues with a small percentage of (1 \rightarrow 4)-linked residues (Bobbit *et al.*, 1977; Buck & Obaidah, 1971; Obaidah & Buck, 1971; Cardemil & Pincheira, 1979; James *et al.* 1990). Furthermore, in *A. fumigatus*, *N. crassa*, and *C. neoformans*, homologs of *S. pombe* α -glucan synthase (Ags1p) have been identified. We therefore predict that also the chemical structure of fission-yeast α -glucan may be conserved among these and other fungi.

Materials and methods

Isolation of cell-wall α -glucan

Cells of strain FH023 (*tr*) (Hochstenbach *et al.*, 1998) were grown in 12 L of YEA medium to a final OD₅₉₅ of 4, cooled in an ice-bath, collected by centrifugation, and washed twice in breaking buffer [5 mM sodium azide, 20 mM Tris-HCl, pH 7.6]. Cells were resuspended in breaking buffer and subjected to mechanical breakage in a Malton-Gaulin, followed by a Bead-Beater (BioSpec Products, Bartlesville, US) by using glass beads (0.45 mm diameter). Twelve rounds of one-minute homogenization were alternated with one-minute cooling periods, such that more than 95% of the cells had lysed. The cell lysate was collected and centrifuged. This and all subsequent centrifugation steps were carried out at 7500 \times at 4 °C for 20 min. After two washing steps in MilliQ-H₂O (Millipore), the pellet was resuspended in 200 ml of SDS-extraction buffer [40 mM 2-mercaptoethanol, 2% (w/v) SDS, 100 mM Na-EDTA, 50 mM Tris-HCl, pH 7.6], and incubated in a boiling waterbath for 20 min to remove cytosolic contaminants. The suspension was centrifuged, washed twice in MilliQ-H₂O, and stored in 5 mM sodium azide at 4 °C.

For α -glucan isolations, whole cell-wall preparations were resuspended in 200 ml of digestion buffer [5 mM sodium azide, 40 mM 2-mercaptoethanol, 50 mM citrate-phosphate, pH 5.3] containing 15 mg of Zymolyase-100T (Seikagaku), and incubated in a rotary shaker at 37 °C for at least 12 h. After centrifugation, the pellet was resuspended in breaking buffer, glass beads were added, and the cell-wall material was treated in a Mikro-Dismembrator (Braun) at 3000 rpm for 3 min to ensure that all cells had been broken. Then, Zymolyase digestion was repeated, followed by a final extraction with SDS. After two washing steps in MilliQ-H₂O, purified α -glucan was stored in 5 mM sodium azide at 4 °C.

Preparation and separation of α -glucan oligosaccharides

100 mg of α -glucan obtained from the cell walls of *S. pombe* wild-type strain FH023 was suspended in digestion buffer [50 mM NaOAc, pH 5.6, 5 mM NaN₃]. *endo*-(1 \rightarrow 3)- α -glucanase (purified from an enzyme preparation from *Trichoderma harzianum* (Novozym, Sigma) via adsorption chromatography) was added and the reaction mixture was

incubated at 37 °C during 1 h. Glucanase digestion was repeated several times using fresh buffer and enzyme. Collected supernatants were desalted by solid-phase extraction using Carbograph SPE columns (Alltech Associates) using the procedure described by Packer *et al.* (1998), which also separates monosaccharides from oligosaccharides. Products were applied on a thermostated Bio-Gel P4 size-exclusion column (1.6 × 90 cm, 55 °C) (BioRad) and eluted with water at a flow-rate of 4.8 ml/h. Carbohydrates in the eluate were quantitatively determined by the phenol-sulfuric acid assay (Dubois *et al.*, 1956). Fractions of 2.0 ml were collected and appropriate fractions were pooled and further purified by HPAEC.

High-performance anion-exchange chromatography

HPAEC was performed on a Dionex DX 500 system equipped with a GP 40 gradient pump and an ED 40 electrochemical detector (Dionex Corporation). A 4 × 250 mm Carbopac PA-1 column was used for analytical HPAEC. Appropriate linear gradients were applied for each component using 100 mM NaOH and 500 mM NaOAc in 100 mM NaOH as eluents. A flow rate of 1.0 ml/min was used. Purification of Bio-Gel P4 fractions was performed on a semi-preparative 9 × 250 mm Carbopac PA-1 column using the same eluents at a flow rate of 4.0 ml/min. Fractions were desalted using Carbograph SPE columns, followed by evaporation of the solvent *in vacuo*.

Nuclear magnetic resonance spectroscopy

¹H-NMR spectra were recorded on a Bruker DRX500 spectrometer (Bijvoet Center, Department of NMR Spectroscopy) at 27 °C. Samples were dissolved in 600 μ l 99.9% D₂O. The residual HOD signal was suppressed by applying a WEFT pulse sequence (Hård *et al.*, 1992). Chemical shifts were referred to internal acetate (¹H: 1.908 ppm). Data were processed using in house developed software.

2-AB labeling, periodate oxidation, and methylation

Oligosaccharides were labeled at their reducing ends with 2-aminobenzamide (2-AB) according to Bigge *et al.* (1995). To the dried oligosaccharides, 5 μ l of a solution of 2-AB (23.6 mg) and sodium cyanoborohydride (31.75 mg) in DMSO/acetic acid 7:3, (500 μ l) was added. The reaction was carried out at 65 °C for 2 h after which the samples were cleaned-up on Whatman QM-A chromatography paper. Reactants were removed by rinsing with acetonitrile (1 ml) and 4% water in acetonitrile (6 × 1 ml). Labeled products were eluted with water (4 × 0.5 ml).

Periodate oxidation of labeled oligosaccharides was basically performed as described by Angel *et al.* (1991). Briefly, 2-AB labeled oligosaccharides were dissolved in 50 mM sodium acetate (pH 5.5) containing 8 mM sodium periodate. Samples were stirred in the dark at 4 °C during 24 h. The pH was adjusted to 7.0 by addition of NaOH. NaBD₄ was added and incubation was continued during 24 h at 4 °C. Excess of NaBD₄ was removed by adjusting the pH to 4.5 with acetic acid. Boric acid was co-evaporated with methanol under reduced

pressure. The reduced products were acetylated in acetic anhydride/pyridine during 30 min at 70 °C. After concentration to dryness, acetylated products were extracted by chloroform from water. The dried products were methylated according to Ciucanu and Kerek (1984).

Mass spectrometry

Experiments were performed on an LC-Q ion trap mass spectrometer (Thermoquest/Finnigan) equipped with a nanoES sample probe (Protana). 2-AB labeled, oxidized/reduced, and per-O-methylated samples were dissolved in methanol/water (7:3) to a concentration of approximately 10 to 30 pmol/ μ l. For each experiment, 2 μ l were loaded into the gold-coated glass capillary. The capillary temperature was set to 180 °C. Spectra were taken in the positive ion mode with a spray voltage of 1.5 kV and a varying capillary voltage of 31.5 to 46.0 V.

References

- Abdel-Akher, M.; Hamilton, J.K.; Montgomery, R. & Smith, F. (1952) A new procedure for the determination of the fine structure of polysaccharides. *J. Am. Chem. Soc.* **74**, 4970-4971.
- Alonso, M.D.; Lomako, J.; Lomako, W.M. & Whelan, W.J. (1995) A new look at the biogenesis of glycogen. *FASEB J.* **9**, 1126-1137.
- Angel, A.S.; Lipniunas, P.; Erlansson, K. & Nilsson, B. (1991) A procedure for the analysis by mass spectrometry of the structure of oligosaccharides from high-mannose glycoproteins. *Carbohydr. Res.* **221**, 17-35.
- Bacon, J.S.D.; Jones, D.; Farmer, V.C. & Webley, D.M. (1968) The occurrence of (1 \rightarrow 3)- α -glucan in *Cryptococcus*, *Schizosaccharomyces* and *Polyporus* species, and its hydrolysis by a *Streptomyces* culture filtrate lysing cell walls of *Cryptococcus*. *Biochim. Biophys. Acta* **158**, 313-315.
- Bigge, J.C.; Patel, T.P.; Bruce, J.A.; Goulding, P.N.; Charles, S.M. & Parekh, R.B. (1995) Nonselective and efficient fluorescent labeling of glycans using 2-amino benzamide and anthranilic acid. *Anal. Biochem.* **230**, 229-238.
- Bobbit, T.F.; Nordin, J.H.; Roux, M.; Revol, J.F. & Marchessault, R.H. (1977) Distribution and conformation of crystalline nigeran in hyphal walls of *Aspergillus niger* and *Aspergillus awamori*. *J. Bacteriol.* **132**, 691-703.
- Buck, K.W. & Obaidah, M.A. (1971) The composition of the cell wall of *Fusicoccum amygdali*. *Biochem. J.* **125**, 461-471.
- Bush, D.A.; Horisberger, M.; Horman, I. & Wursch, P. (1974) The wall structure of *Schizosaccharomyces pombe*. *J. Gen. Microbiol.* **81**, 199-206.
- Cardemil, L. & Pincheira, G. (1979) Characterization of the carbohydrate component of fraction I in the *Neurospora crassa* cell wall. *J. Bacteriol.* **137**, 1067-1072.
- Ciucanu, I. & Kerek, F. (1984) A simple and rapid method for the permethylation of carbohydrates. *Carbohydr. Res.* **131**, 209-217.
- Costello, C.E. (1997) Time, life...and mass spectrometry. New techniques to address biological questions. *Biophys. Chem.* **68**, 173-188.

- Dell, A. & Morris, H.R. (2001) Glycoprotein structure determination by mass spectrometry. *Science* **291**, 2351-2356.
- Dell, A.; Morris, H.R.; Panico, M.; Haslam, S.M.; Easton, R. & Khoo, K.-H. (1997) Trends in mass spectrometry of carbohydrates and glycoconjugates. *Carbohydr. Eur.* **17**, 10-16.
- Domon, B. & Costello, C.E. (1988) A systematic nomenclature for carbohydrate fragmentation in FAB-MS/MS spectra of glycoconjugates. *Glycoconj. J.* **5**, 379-409.
- Dubois, M.; Gilles, K.A.; Hamilton, J.K.; Rebers, P.A. & Smith, F. (1956) Colorimetric method for the determination of sugars and related substances. *Anal. Chem.* **28**, 350-356.
- Dyer, J.R. (1956) Use of periodate oxidation in biochemical analysis. In: *Methods of biochemical analysis*; Glick, D., Ed.; Vol. 3, Interscience Publishers Inc.: New York, pp. 111-152.
- Fox, J.; Kawaguchi, K.; Greenberg, E. & Preiss, J. (1976) Biosynthesis of bacterial glycogen. Purification and properties of the *Escherichia coli* B ADPglucose:1→4- α -D-glucan 4- α -glucosyltransferase. *Biochemistry* **15**, 849-856.
- Fuglsang, C.C.; Berka, R.M.; Wahleithner, J.A.; Kauppinen, S.; Shuster, J.R.; Rasmussen, G. Halkier, T.; Dalboge, H. & Henrissat, B. (2000) Biochemical analysis of recombinant fungal mutanases. A new family of α 1→3-glucanases with novel carbohydrate-binding domains. *J. Biol. Chem.* **275**, 2009-2018.
- Germaine, G.R.; Chludzinski, A.M. & Schachtele, C.F. (1974) *Streptococcus mutans* dextransucrase: requirement for primer dextran. *J. Bacteriol.* **120**, 287-294.
- Hård, K.; Van Zadelhoff, G.; Moonen, P.; Kamerling, J.P. & Vliegthart, J.F.G. (1992) The Asn-linked carbohydrate chains of human Tamm-Horsfall glycoprotein of one male. Novel sulfated and novel N-acetylgalactosamine-containing N-linked carbohydrate chains. *Eur. J. Biochem.* **209**, 895-915.
- Hochstenbach, F.; Klis, F.M.; Van Den Ende, H.; Van Donselaar, E. Peters, P.J. & Klausner, R.D. (1998) Identification of a putative α -glucan synthase essential for cell wall construction and morphogenesis in fission yeast. *Proc. Natl. Acad. Sci. U S A* **95**, 9161-9166.
- James, P.G.; Cherniak, R.; Jones, R.G. & Stortz, C.A. (1990) Cell-wall glucans of *Cryptococcus neoformans* Cap 67. *Carbohydr. Res.* **198**, 23-38.
- Kawaguchi, K.; Fox, J.; Holmes, E.; Boyer, C. & Preiss, J. (1978) *De novo* synthesis of *Escherichia coli* glycogen is due to primer associated with glycogen synthase and activation by branching enzyme. *Arch. Biochem. Biophys.* **190**, 385-397.
- Lindberg, B. (1972) Methylation analysis of polysaccharides. In: *Methods in enzymology*; Ginsburg, V., Ed.; Academic Press: New York and London; Vol. 28; pp. 178-195.
- Obaidah, M.A. & Buck, K.W. (1971) Characterization of two cell-wall polysaccharides from *Fusicoccum amygdali*. *Biochem. J.* **125**, 473-480.
- Packer, N.H.; Lawson, M.A.; Jardine, D.R. & Redmond, J.W. (1998) A general approach to desalting oligosaccharides released from glycoproteins. *Glycocon. J.* **15**, 737-747.
- Peng, L.; Kawagoe, Y.; Hogan, P. & Delmer, D. (2002) Sitosterol- β -glucoside as primer for cellulose synthesis in plants. *Science* **295**, 147-150.
- Smith, A.M. (1999) Making starch. *Curr. Opin. Plant. Biol.* **2**, 223-229.
- Whelan, W.J. (1998) Pride and prejudice: the discovery of the primer for glycogen synthesis. *Protein Sci.* **7**, 2038-201.

